CHIN. PHYS. LETT. Vol. 33, No. 3 (2016) 037401

Single Crystal Growth and Physical Property Characterization of Non-centrosymmetric Superconductor $PbTaSe_2$ *

Yu-Jia Long(龙雨佳)[1,2], Ling-Xiao Zhao(赵凌霄)[2], Pei-Pei Wang(王培培)[2], Huai-Xin Yang(杨槐馨)[2], Jian-Qi Li(李建奇)[2,3], Hai Zi(子海)[2], Zhi-An Ren(任治安)[2], Cong Ren(任聪)[2]**, Gen-Fu Chen(陈根富)[1,2,3]**

[1] *Department of Physics, Renmin University of China, Beijing 100872*

[2] *National Laboratory for Superconductivity, Institute of Physics and Beijing National Laboratory for Condensed Matter Physics, Chinese Academy of Sciences, Beijing 100190*

[3] *Collaborative Innovation Center of Advanced Microstructures, Beijing 100190*

(Received 4 December 2015)

We report on the single crystal growth and superconducting properties of $PbTaSe_2$ with the non-centrosymmetric crystal structure. By using the chemical vapor transport technique, centimeter-size single crystals are successfully obtained. The measurement of temperature dependence of electrical resistivity $\rho(T)$ in both normal and superconducting states indicates a quasi-two-dimensional electronic state in contrast to that of polycrystalline samples. Specific heat $C(T)$ measurement reveals a bulk superconductivity with $T_c \simeq 3.75\,K$ and a specific heat jump ratio of 1.42. All these results are in agreement with a moderately electron–phonon coupled, type-Ⅱ Bardeen–Cooper–Schrieffer superconductor.

PACS: 74.25.−q, 74.62.Bf, 74.20.Rp DOI: 10.1088/0256-307X/33/3/037401

Non-centrosymmetric superconductors (NCSs) are those materials that lack an inversion center in crystal structure, and therefore, it is possible that non-centrosymmetric superconductors might host exotic superconductivity whose origin cannot be explained by electron–phonon interactions within the framework of the Bardeen–Cooper–Schrieffer (BCS) theory. In non-centrosymmetric superconductors, it has been predicted that a mixed spin-singlet/triplet pairing state exists due to the strong spin–orbit splitting in the absence of inversion symmetry.[1] Despite an intense search for NCS, until now only a few such materials are known, such as $CePt_3Si$, Ru_7B_3 and Li_2Pt_3B,[2−6] and their superconducting properties have been checked concerning the interesting physics issues. For several materials such as Li_2Pt_3B, U_2PtC_2, a spin triplet component of the superconducting order parameter has been detected by nuclear magnetic resonance as well as magnetic penetration depth experiment, etc.[7−11] On the other hand, specific heat and magnetic penetration depth measurements on Ru_7B_3, Re_3W, $Ca(Ir/Pt)Si_3$ and Li_2Pd_3B indicate a fully gapped superconducting state, which can be described in the framework of a singlet s-wave BCS theory.[6,12−17] However, all these experiments were performed on oriented polycrystalline samples, and the study of the intrinsic characteristics of NCSs was hindered by the preparation of high quality single crystal.

Very recently, Ali *et al.* reported the discovery of superconductivity on polycrystalline $PbTaSe_2$, which crystallizes in a layered structure with Pb and $TaSe_2$ layers stacked alternatively.[18] In such samples, the Ta atom deviated from the symmetry center and thus forms a non-centrosymmetric structure. In addition, the heavy atom mass of Ta with $5d$ electron state might introduce strong spin-orbit coupling (SOC), an ingredient of topological superconductivity.[19] Thus a detailed investigation of the pairing symmetry of this compound is very attractive. Nevertheless, $PbTaSe_2$ polycrystalline shows a metal-like behavior and critical transition temperature is about 3.8 K. Specific heat measurement shows that $\Delta C/\gamma T_c$ is about 1.41, close to 1.43 forecasted by conventional BCS superconductivity. To explore the intrinsic physical property of $PbTaSe_2$, high quality $PbTaSe_2$ single crystal is crucial. In this work, we focus on the growth of high quality $PbTaSe_2$ single crystals, and the characterization of its intrinsic properties of both the normal and superconducting states. The preliminary experimental results point to $PbTaSe_2$ being a singlet s-wave BCS superconductor in moderate coupling strength.

High-quality single crystals of $PbTaSe_2$ were grown by chemical vapor transport by using iodine as a transport agent. The polycrystalline $PbTaSe_2$ was first synthesized via a solid state reaction of high purity Ta powder, PbSe precursor, and $TaSe_2$ precursor in an evacuated quartz tube at 820℃ for 50 h. Then, the obtained materials were ground, sealed in an evacuated quartz tube with iodine concentration of 3 mg/cm^3,

*Supported by the National Basic Research Program of China under Grant Nos 2015CB921303, 2011CBA00100 and 2012CB821404, the Strategic Priority Research Program (B) of Chinese Academy of Sciences under Grant Nos XDB07020100 and XDB07020200, and the National Natural Science Foundation of China under Grant No 11174350.

**Corresponding author. Email: cong_ren@iphy.ac.cn; gfchen@iphy.ac.cn

© 2016 Chinese Physical Society and IOP Publishing Ltd

heated in a two-zone furnace for two weeks. The optimal hot and cold zone temperatures were 820℃ and 770℃, respectively.

The resulting crystals of $PbTaSe_2$ are extremely thin plates with triangular shape and atomic-flatness surface. The typical dimensions of $PbTaSe_2$ are $10 \times 10 \times 0.005\,mm^3$, and are very easily cleaved along the c-axis, as shown in the center panel of Fig. 1(a). The obtained crystals were characterized by x-ray diffraction (XRD) by using a PANalytical diffractometer with Cu Kα radiation at room temperature. Figure 1(b) shows the XRD pattern for an as-grown single crystal with the $(00l)$ reflections with the full-width-at-half-maximum around 0.1°. The lattice constant $c = 9.38$ Å was calculated from the higher order peaks. The atomic ratio determined from energy-dispersive x-ray (EDX) spectroscopy (Fig. 1(c)) is very close to 1:1:2 (Pb:Ta:Se).

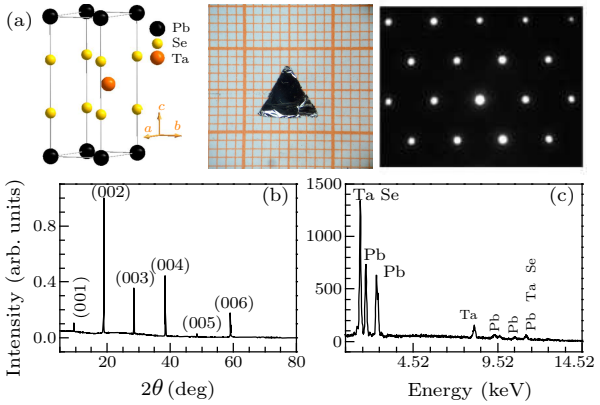

Fig. 1. (Color online) (a) Left panel: the crystal structure of $PbTaSe_2$. Center panel: the typical triangle plate-like crystal with dimension of $10 \times 10 \times 0.005\,mm^3$. Right panel: the selected area electron diffraction (SAED) pattern of $PbTaSe_2$. (b) The x-ray diffraction (XRD) pattern of $PbTaSe_2$ single-crystal taken at room temperature. (c) EDX spectrogram of $PbTaSe_2$.

The properties of both normal and superconducting states are examined through temperature-dependent measurements of the dc magnetic susceptibility $\chi(T)$ and electrical resistivity $\rho(T)$ by using a PPMS system (Quantum Design). Figure 2(a) shows the superconducting transition characterized by dc susceptibility with magnetic field parallel to the a–b plane. As shown, the superconducting transition is identified as the onset of χ at T_c=3.75 K. A portion of 40% field-cooling (FC) χ_{FC} in the normalized zero-field-cooling (ZFC) signal indicates few pinning centers for the vortices, suggesting high homogeneity and less twinned boundary in our samples. The temperature-dependent resistivity $\rho(T)$ provides rich information about the physical properties of $PbTaSe_2$ crystal. As shown in the inset of Fig. 2(b) the superconducting transition temperature 3.85 K is identified as the middle point of the transition regime, in good agreement with the value determined in diamagnetic response (Fig. 2(a)). The temperature dependence of the in-plane ρ_{ab} and out-of-plane ρ_c resistivities for $PbTaSe_2$ are displayed in Figs. 2(b) and 2(c), respectively. Both ρ_{ab} and ρ_c show a Fermi liquid behavior: linearly decreased $\rho - T$ behavior at high T and saturated finite $\rho - T^n$ at low T. The residual resistivity ratio [RRR $\equiv \rho(300\,K)/4\,K$] of ρ_{ab} is about 290 with a residual resistivity $\rho_{ab}(4\,K) \simeq 0.14\,\mu\Omega\cdot cm$. It is noted that RRR for a polycrystalline $PbTaSe_2$ is less than 10 with a large residual resistivity.[18] Comparatively, RRR for ρ_c is about 55 for the same crystal, and $\rho_c(4\,K)$ is 0.27 mΩ cm, more than three orders of magnitude higher than $\rho_{ab}(4\,K)$. The normal-state resistivity anisotropy of $\rho_c(T)/\rho_{ab}(T)$ is comparable with that of layered cuprates Bi2212,[20] implying that $PbTaSe_2$ has quasi-two-dimensional electronic states, as expected due to the layered crystal structure.

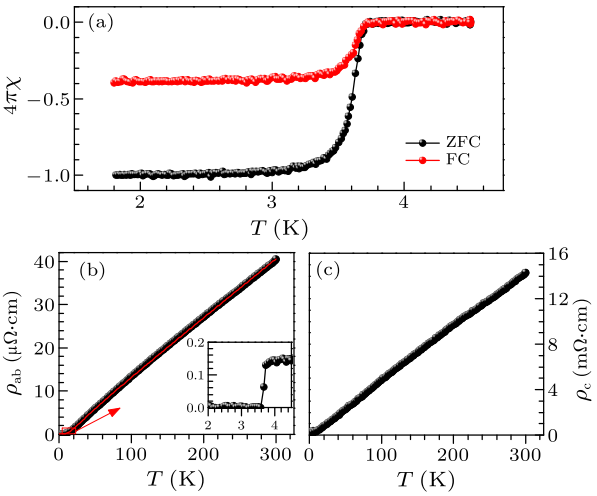

Fig. 2. (Color online) (a) The dc susceptibility χ as a function of temperature in field-cooling (FC) and zero-field-cooling (ZFC) modes under a dc magnetic field of $H_{dc} = 5$ Oe for H_{dc} parallel to the a–b plane. The data are normalized with the criterion $\chi_{ZFC}(0) = -1/4\pi$. The superconducting transition temperature T_c is determined as the onset of χ. Temperature dependence of electrical resistivity of $PbTaSe_2$ for currents flowing (b) in the a–b plane (ρ_{ab}) and (c) along the c-axis (ρ_c). The red solid line in Fig. 2(b) is the fit to the $\rho_{ab} - T$ data by using Eq. (1). The inset of Fig. 2(b) is the expanded view of ρ_{ab} around the superconducting transition.

The linearly T-dependent ρ_{ab} and high RRR are the manifestation of the dominance of electron–phonon scattering in the resistivity mechanism, and allow us to estimate the Debye temperature Θ_D, which characterizes the lattice thermal vibration energy. Based on the famous Bloch–Grüneisem formula, the ρ-T curve can be described as

$$\rho(T) = \rho_0 + A\left(\frac{T}{\Theta_D}\right)^5 \cdot \int_0^{\Theta_D/T} \frac{x^5 dx}{[\exp(x) - 1][1 - \exp(-x)]}, \quad (1)$$

where A is a constant in μΩ·cm related to the electron–phonon coupling strength. Excellent fitting to the $\rho_{ab}(T)$ curve in the whole T region is obtained, as shown in the main panel of Fig. 2(b), yielding $\Theta_D \simeq 88$ K and $A = 45$ μΩ·cm.

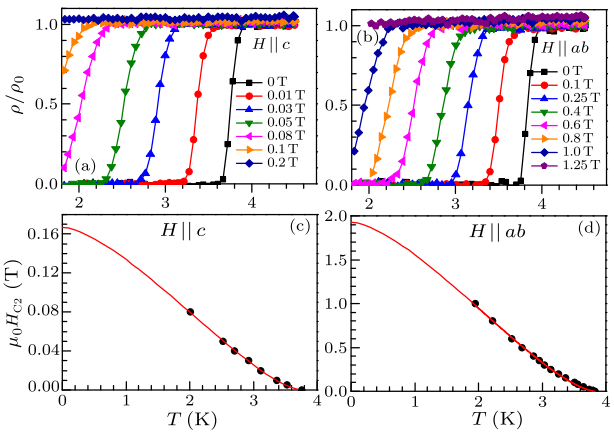

Fig. 3. (Color online) Temperature dependence of the in-plane electrical resistivity for $PbTaSe_2$ in different magnetic fields with (a) $H\|c$ and (b) $H\|ab$, and the extracted values of H_{c2} as a function of temperature for (c) $H\|c$ and (d) $H\|ab$.

The upper critical magnetic field H_{c2} of a superconductor and its anisotropy measure the strength of superconductivity in response to external magnetic fields, which gives clues to the superconducting Cooper pairing. Temperature dependence of in-plane resistivity for $PbTaSe_2$ in various magnetic fields with $H\|c$ and $H\|ab$ are shown in Figs. 3(a) and 3(b), respectively. Superconducting transition shifts to low temperature with increasing the magnetic field, which was particularly significant when H is parallel to the c-direction. We choose T_c^{middle} as the critical temperature and construct the $\mu_0 H_{c2}$–T curves for $H\|c$ and $H\|ab$, respectively, as shown in Figs. 3(c) and 3(d). It is noted that the $\mu_0 H_{c2}$–T curves exhibit an anomalous upward curvature at $T \to T_c$. It was suggested to be related to the multi-band nature. Further investigations are required to identify the underlying mechanism.

The upper critical field $H_{c2}(0)$ can be roughly estimated by using the previously proposed formula $H_{c2}(T) = H_{c2}(0)(1 - t^{3/2})^{3/2}$, in which $t = T/T_c$,[21] as shown in Figs. 3(c) and 3(d) for $H\|c$ and $H\|ab$, respectively. In this T-region ($0.46 < t \leq 1$), $\mu_0 H_{c2}^c(0)$ ~0.17 T and $\mu_0 H_{c2}^{ab}(0)$ ~1.93 T. Thus the anisotropic $\Gamma = \frac{H_{c2}^{ab}(0)}{H_{c2}^{c}(0)} = \sqrt{\frac{m_c^*}{m_{ab}^*}} = 11.6$, where m_c^* and m_{ab}^* mean the effective mass of the carriers along the c-axis and the ab-plane.[22] For a pairing symmetry test, the value of $\mu_0 H_{c2}^{ab}(0) = 1.93$ T is much lower than the Pauli paramagnetic limit, $\mu_0 H_P = 1.86 T_c = 7$ T, implying that the orbital effect dominates in limiting its H_{c2}.

Using the obtained $H_{c2}(0)$ values, the basic parameters of superconductor coherent length ξ is estimated based on the Ginzburg–Landau formula: $H_{c2}^c(0) = \phi_0/2\pi\xi_{ab}^2(0)$ and $H_{c2}^{ab}(0) = \phi_0/2\pi\xi_{ab}(0)\xi_c(0)$, where ϕ_0 is the magnetic flux quantum. Here for $PbTaSe_2$, $\xi_{ab} = 44.4$ nm and $\xi_c = 3.84$ nm as calculated.

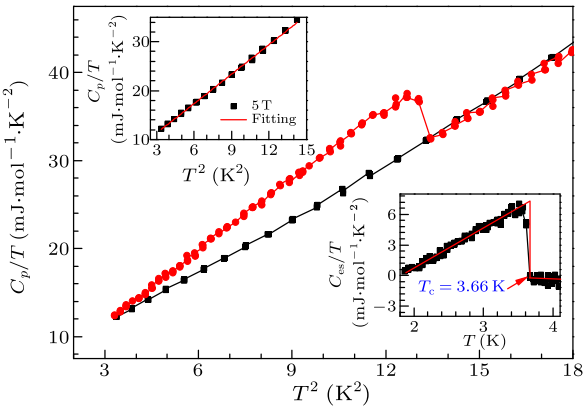

Fig. 4. (Color online) Raw data of specific heat C_p/T as a function of T^2 in $\mu_0 H = 0$ (red solid symbols) and 5 Tesla (black solid symbols). Left upper inset: specific heat data in 5 T (normal state) (black solid symbols) with their fit by relation $C/T = \gamma_n + \beta T^2$. Right lower inset: temperature dependence of $C/T(H = 0) - C/T(\mu_0 H = 5T)$ around the superconducting transition region. The jump in specific heat is the manifestation of superconducting transition, and thus the bulk T_c can be determined as the onset of the specific heat jump.

Table 1. The superconducting and normal-state parameters of the non-centrosymmetric material $PbTaSe_2$.

Parameters	$PbTaSe_2$
ρ_{ab} (μΩ·cm) (4 K)	0.14
ρ_c (mΩ·cm) (4 K)	0.27
γ_n (mJ/mol·K^2)	5.3
β (mJ/mol·K^4)	2.01
Θ_D (K)	157
$\mu_0 H_{c2}^{ab}(0)$ (T)	1.93
$\mu_0 H_{c2}^{c}(0)$ (T)	0.17
ξ_{ab} (nm)	44.4
ξ_c (nm)	3.84
Γ	11.6

Specific heat C_p measurements were carried out at $\mu_0 H$=0 and 5 T ($H\|c$-axis) for $PbTaSe_2$, and the data are illustrated in Fig. 4. At zero field, a specific jump near T_c is very sharp, indicating the good quality of the sample. To clearly resolve the specific heat jump with respect to its normal state value, we apply a field of $\mu_0 H$=5 T to fully suppress the superconductivity, as shown in the left upper inset of Fig. 4. The data of C_p/T as a function of T^2 for $PbTaSe_2$ can be well fitted by the formula $C_p = \gamma_n T + \beta T^3$, indicating that the specific heat C_p is mainly contributed by electron and phonon terms in the T region. The fit to the data yields electronic coefficient $\gamma_n = 5.3$ mJmol^{-1}K^{-2}, and phonon specific heat coefficient $\beta = 2.01$ mJmol^{-1}K^{-4}. Thus the Debye temperature Θ_D is estimated to be 157 K

by using $\Theta_{\rm D} = (12\pi^4 nR/5\beta)^{1/3}$ with $n = 4$ and $R = 8.31$. Here the obtained $\Theta_{\rm D}$ is about twice that obtained from the $\rho - T$ measurement. We argue that Debye energy accounts for the pure phonon system, regardless of the electron system. Thus the Debye temperature obtained from specific heat measurement is more accurate compared with that obtained from the $\rho - T$ measurement. Therefore, using $\gamma_n = 5.3\,{\rm mJmol^{-1}K^{-2}}$ and $T_{\rm c} = 3.7\,{\rm K}$, we obtain $\Delta C/\gamma_n T_{\rm c} = 1.425$, close to the value of 1.43 within the BCS weak-coupling approximation. Furthermore we can estimate the electron–phonon coupling constant $\lambda_{\rm e-ph}$ following the McMillan equation:[23] $\lambda_{\rm e-ph} = \frac{1.04+\mu^* \ln(\Theta_{\rm D}/1.45T_{\rm c})}{(1-0.62)\mu^* \ln(\Theta_{\rm D}/1.45T_{\rm c})-1.04}$, where μ^* is the Coulomb pseudopotential assigned a value of 0.13.[24] We obtain $\lambda_{\rm e-ph} = 0.73$. For comparison, for strong coupling superconductors, such as Pb, $\lambda_{\rm e-ph} \sim 1.12$; and $\lambda_{\rm e-ph} \sim 0.36$ for indium in the weak-coupling limit.[24] This is similar to other moderately coupled superconductors. In Table 1 we list the superconducting and normal-state parameters of the non-centrosymmetric material $PbTaSe_2$. Future efforts are strongly desired to investigate the origin of the H_{c2} anomaly.

In summary, we have successfully grown $PbTaSe_2$ single crystals with high quality through the chemical iodine-vapor transport method. The physical properties of both normal and superconducting states are characterized by resistivity and heat capacity measurements. All these results point to $PbTaSe_2$ a two-dimension, moderately electron–phonon coupled type-Ⅱ BCS superconductor.

As preparing this manuscript, we became aware of the related studies reporting the growth and characterization of $PbTaSe_2$ single crystals (arXiv:1511.05295), similar to the results we reported here.

References

[1] Bauer E and Sigrist M (ed) 2012 *Non-Centrosymmetric Superconductors: Introduction and Overview* (Berlin: Springer) vol 847 p 129

[2] Togano K, Badica P, Nakamori Y, Orimo S, Takeya H and Hirata K 2004 *Phys. Rev. Lett.* **93** 247004

[3] Badica P, Kondo T, Kudo T, Nakamori Y, Orimo S and Togano K 2004 *Appl. Phys. Lett.* **85** 4433

[4] Badica P, Kondo T and Togano K 2005 *J. Phys. Soc. Jpn.* **74** 1014

[5] Bauer E, Hilscher G, Michor H, Paul C, Scheidt E W, Gribanov A, Seropegin Y, Noël H, Sigrist M and Rogl P 2004 *Phys. Rev. Lett.* **92** 027003

[6] Fang L, Yang H, Zhu X Y, Mu G, Wang Z S, Shan L, Ren C and Wen H H 2009 *Phys. Rev.* B **79** 144509

[7] Yuan H Q, Agterberg D F, Hayashi N, Badica P, Vandervelde D, Togano K, Sigrist M and Salamon M B 2006 *Phys. Rev. Lett.* **97** 017006

[8] Nishiyama M, Inada Y and Zheng G Q 2007 *Phys. Rev. Lett.* **98** 047002

[9] Eguchi G, Peets D C, Kriener M, Yonezawa S, Bao G, Harada S, Inada Y, Zheng G Q and Maeno Y 2013 *Phys. Rev.* B **87** 161203

[10] Harada S, Zhou J J, Yao Y G, Inada Y and Zheng G Q 2012 *Phys. Rev.* B **86** 220502(R)

[11] Mounce A M, Yasuoka H, Koutroulakis G, Ni N, Bauer E D, Ronning F and Thompson J D 2015 *Phys. Rev. Lett.* **114** 127001

[12] Nishiyama M, Inada Y and Zheng G Q 2005 *Phys. Rev.* B **71** 220505(R)

[13] Khasanov R, Landau I L, Baines C, La Mattina F, Maisuradze A, Togano K and Keller H 2006 *Phys. Rev.* B **73** 214528

[14] Biswas P K, Hillier A D, Lees M R and Paul D M 2012 *Phys. Rev.* B **85** 134505

[15] Singh R P, Hillier A D, Chowdhury D, Barker J A T, Paul D M, Lees M R and Balakrishnan G 2014 *Phys. Rev.* B **90** 104504

[16] Eguchi G, Peets D C, Kriener M, Maeno Y, Nishibori E, Kumazawa Y, Banno K, Maki S and Sawa H 2011 *Phys. Rev.* B **83** 024512

[17] Frandsen B A, Cheung S C, Goko T, Liu L, Medina T, Munsie T S J, Luke G M, Baker P J, Jimenez S M P, Eguchi G, Yonezawa S, Maeno Y and Uemura Y J 2015 *Phys. Rev.* **91** 014511

[18] Ali M N, Gibson Q D, Klimczuk T and Cava R J 2014 *Phys. Rev.* B **89** 020505(R)

[19] Sasaki S, Ren Z, Taskin A A, Segawa K, Fu L and Ando Y 2012 *Phys. Rev. Lett.* **109** 217004

[20] Motohashi T, Nakayama Y, Fujita T, Kitazawa K, Shimoyama J and Kishio K 1999 *Phys. Rev.* B **59** 14080

[21] Micnas R, Ranninger J and Robaszkiewicz S 1990 *Rev. Mod. Phys.* **62** 113

[22] Klemm R A and Clem J R 1980 *Phys. Rev.* B **21** 1868

[23] McMillan W L 1968 *Phys. Rev.* **167** 331

[24] Poole Jr C P 2000 *Handbook of Superconductivity* (San Diego: Academic Press) pp 478–479